vehicles

MDPI

Article

Implementation of an Integrated System for Preventive Maintenance Management and Alerts in Light Vehicles

Joseph Barreiro-Zambrano, Juan Martinez-Parrales and Roberto López-Chila *

Grupo de Innovación Educativa Tecnologías de la Información y Comunicaciones en el Proceso de Enseñanza-Aprendizaje (GIE-TICEA) and Grupo de Investigación en Movilidad Inteligente (GMOVINT) Research Groups, Automotive Engineering Career, Politecnica Salesiana University, Guayaquil 090109, Ecuador; jbarreiroz@est.ups.edu.ec (J.B.-Z.); jmartinezp4@est.ups.edu.ec (J.M.-P.)
* Correspondence: rlopezch@ups.edu.ec

Abstract

Inadequate vehicle maintenance management is one of the main causes of road accidents and elevated operating costs in light vehicles. This paper addresses this problem through the development and implementation of a low-cost integrated system for preventive maintenance management and alerts. The device, based on an open-hardware architecture (Arduino Mega 2560), integrates Global Positioning System (GPS) and mobile communication (GSM/LTE) modules to monitor distance traveled in real time and notify the user via SMS about the proximity of critical services such as oil changes, brake inspections, and timing-belt replacements. Its technical contribution lies in the integration of non-intrusive virtual ignition, filtered GPS-based odometry, configurable MicroSD-based persistence, and progressive SMS alert logic into a low-cost aftermarket system for conventional vehicles without OBD-II dependence. Experimental validation was conducted in the city of Guayaquil using a 2012 Hyundai Accent. Field tests were carried out in three scenarios: a dense urban route, a peripheral road, and interurban routes. Results showed satisfactory accuracy with a global average percentage error of 3.98% compared to the vehicle's odometer and 100% effectiveness in sending alerts under the tested conditions (20/20 events; exact 95% binomial confidence interval: 83.2–100.0%). These results provide strong evidence of technical feasibility for the proposed architecture under the tested conditions in a representative single-vehicle proof-of-concept, while broader cross-vehicle validation remains necessary before generalizing the system to the wider diversity of aging fleets.

Keywords: preventive maintenance; Arduino; GPS; GSM; vehicle telemetry; road safety

Check for updates

Received: 20 March 2026
Revised: 26 April 2026
Accepted: 28 April 2026
Published: 1 May 2026

Copyright: © 2026 by the authors. Licensee MDPI, Basel, Switzerland. This article is an open access article distributed under the terms and conditions of the Creative Commons Attribution (CC BY) license.

1. Introduction

In the technical management of light vehicles, preventive maintenance represents a strategy aimed at anticipating mechanical failures and keeping operational performance within safe parameters. At the global level, inadequate management of service intervals is a precursor to critical mechanical failures, which represent a significant cause of road accidents [1]. In the Ecuadorian context, this problem acquires a structural dimension due to the characteristics of the vehicle fleet. According to the Annual Report of the Automotive Sector by AEADE, the national vehicle fleet shows a marked aging trend: 75% of vehicles are more than six years old, and 60% exceed eleven years of use [2].

This statistical reality reveals a substantial technological gap. The vast majority of these vehicles, manufactured before the mass adoption of consumer telematics, lack native

maintenance-alert systems, forcing owners to rely on manual methods that are prone to the "forgetfulness factor" [3]. Technological obsolescence not only increases operating costs due to corrective repairs [4] but also has direct environmental implications. National regulations such as RTE-002 of INEN [5] establish strict emission control limits; however, the technical literature warns that internal combustion engines are primary sources of harmful substances such as carbon monoxide (CO), carbon dioxide (CO_2), and nitrogen oxides (NO_x) [6]. Consequently, when these engines operate without adequate maintenance (oil changes, filters, or spark plugs), their operation deviates from optimal design parameters, compromising regulatory compliance and worsening air quality.

Although the recent literature proposes OBD-II-based monitoring solutions and cloud-based platforms, the landscape of low-cost vehicular monitoring alternatives is broader than conventional proprietary telematics alone. In addition to ECU-dependent systems, recent studies have explored low-cost OBD-II interfaces for vehicle-data acquisition and analysis, while other approaches rely on LPWAN-oriented communication schemes for reduced operating cost and extended deployment flexibility. However, these alternatives generally remain dependent on diagnostic-port compatibility, mobile-device availability, or external communication infrastructure. In aging or compatibility-limited vehicles, these factors may still create cost or usability barriers for the average user of a conventional M1 category vehicle. These alternatives define a broader technological landscape in which the present work should be situated, particularly when comparing trade-offs among cost, connectivity, diagnostic depth, and installation independence from the vehicle bus. There is therefore a need to develop complementary aftermarket solutions that do not rely exclusively on OBD-II access [7–11].

Additionally, recent studies have shown that real urban traffic conditions in congested cities such as Guayaquil exhibit high dynamic variability and a complex urban morphology characterized by high building density and "urban canyon" effects that hinder the propagation of wireless signals [12]. This limits the representativeness of measurements obtained under controlled scenarios or standardized cycles, making experimental validation of vehicular systems—especially those relying on GPS/GSM telemetry—necessary directly on real traffic routes [6].

This work addresses this need through the implementation of an integrated preventive maintenance management and alert system. The device uses an open-hardware architecture (Arduino Mega) and GSM (Global System for Mobile Communications) communication via SMS (Short Message Service), technologies selected for their high availability and low operating cost [13]. The objective is to validate a prototype capable of calculating the distance traveled via GPS and autonomously notifying the user about the proximity of critical services, bridging the technological gap in the vehicle fleet and contributing to road safety.

The main contribution of this work does not lie in the mere use of commercial modules, but in the development and experimental validation of a non-intrusive low-cost preventive maintenance architecture for conventional light vehicles. The proposed system combines filtered GPS-based odometry adapted to stop-and-go traffic, voltage-based virtual ignition detection that avoids intrusive connection to the ACC line, configurable MicroSD-based persistence for vehicle data and recovery after power interruptions, and a progressive SMS alert strategy for anticipatory maintenance scheduling. In this way, the system extends preventive maintenance digitization to aging vehicle fleets that lack native telematics and cannot be reliably served by OBD-II-dependent solutions.

2. Materials and Methods

The materials used and the methodological procedure for developing and validating the proposed system are presented below.

2.1. Research Design

The study was structured as a technical prototype–validation design with pre/post instrumentation comparison, rather than as a behavioral intervention study [14]. The baseline phase consisted of recording mileage conventionally via the vehicle odometer, used as the operational reference, while the post-implementation phase evaluated the behavior of the proposed electronic system in terms of automatic distance measurement, alert triggering, and subsystem functionality. The vehicle, habitual routes, and general operating conditions were kept constant during both phases in order to compare measurement coherence and technical performance before and after the instrumentation change. The unit of analysis consisted of a single M1 category light vehicle, and the experimental period lasted approximately five weeks, which was sufficient for engineering validation of the prototype but not for observing long-term maintenance-compliance behavior under natural use conditions.

2.2. Methodological Approach Oriented Toward Operational Optimization

Preventive maintenance optimization is approached from an operational perspective, understood as an improvement in the reliability and timeliness of the information used to schedule technical interventions. In this sense, digitizing monitoring constitutes a key element for reducing uncertainty in planning and strengthening data-driven decision-making. Recent studies on condition-based maintenance indicate that the incorporation of digital tracking systems helps improve operational efficiency by providing continuous and verifiable information [15]. It has also been reported that the integration of electronic monitoring tools can increase control precision and reduce unplanned events in maintenance processes [16].

Consistent with this conceptual framework, the developed system was designed to automate mileage control, reduce dependence on manual logging, and improve the timeliness of service alerts. The implemented operational sequence and the decision criteria adopted are represented schematically in Figure 1. The optimization considered therefore corresponds to a functional improvement in preventive maintenance control, supported by the availability of quantifiable real-time information.

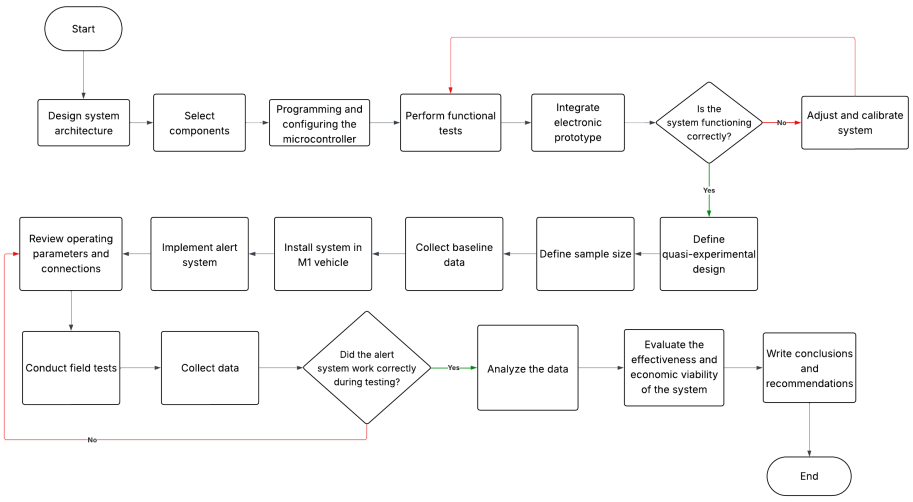

Figure 1. Methodological flowchart of the system.

2.3. Unit of Analysis and Testing Environment

Experimental tests were carried out in the city of Guayaquil, Ecuador, selected for its heterogeneous traffic conditions and dense urban topography. According to prior studies on driving cycles in this locality, the variability of stops and the built environment create a challenging scenario for satellite signal stability, known as the "urban canyon" effect [6,7]. These conditions allow evaluation of the robustness of the prototype's filtering algorithm against momentary precision losses.

The unit of analysis consisted of an M1 category light vehicle (sedan). A 2012 Hyundai Accent with an initial odometer reading of 145,230 km was selected, as it is representative of the majority segment of the national vehicle fleet according to AEADE [2]. Accordingly, the present experimental validation should be interpreted as a single-vehicle proof-of-concept in a representative aging light vehicle, rather than as a complete demonstration of cross-vehicle generalizability.

For distance validation, the vehicle's digital odometer was adopted as the operational reference rather than as an independent metrological ground truth. This decision is grounded in the functional coherence of the system: since maintenance intervals are defined and perceived by the user from the dashboard reading, the practically relevant comparison metric is the odometer and not an absolute geodetic measurement. To reduce one of the main physical factors affecting odometer behavior, tire pressure was standardized at 30 PSI before each test. In this context, the NIST 4% odometer tolerance was used only as a contextual benchmark for practical acceptability and not as an independent validation of the odometer itself [17].

Furthermore, the legal acceptance tolerance for commercial odometers, established at 4% by the National Institute of Standards and Technology (NIST) [18], was considered as a control limit for evaluating prototype performance.

This interpretation is also consistent with recent work on traffic speed behavior in urban environments, where highly variable and congested operating conditions are recognized as a major source of complexity for speed-related modeling and prediction. Such variability provides additional context for the stop-and-go dynamics observed in dense urban corridors and helps explain why GPS-based odometry is more sensitive to residual drift and signal perturbations under these conditions [19].

2.4. Materials and System Components

The system is based on a modular open-hardware architecture, validated in the literature for its cost-effectiveness [20]. An Arduino Mega 2560 microcontroller was used, chosen for its capacity to handle multiple simultaneous serial ports for GPS and GSM [21]. A Ublox Neo 6M GPS module with concurrent tracking capability was integrated, which improves precision in urban environments [22]. An A7670SA GSM module was employed for transmitting alerts via SMS. This architecture guarantees a higher delivery rate in areas with intermittent coverage and reduces monthly operating costs by 75–85% compared to mobile data solutions [23,24]. A voltage sensor for detecting vehicle ignition status, and a MicroSD card reader module for local data storage, were also included. In the current implementation, DATA.CSV is treated as a static read-only database, whereas CONFIG.TXT stores the dynamic user state. When state persistence is triggered, the firmware rewrites CONFIG.TXT as a complete state snapshot and explicitly closes the file at the end of the write cycle. The cost details and specifications of the components used are shown in Table A2.

Logical development and data analysis were supported by specialized software tools. Microcontroller firmware was programmed in the Arduino IDE version 2.3.7 integrated development environment, using C++ for managing positioning and communication

libraries. For schematic design and pre-experimental circuit validation (see complete diagram in Figure A1 and connections in Table A1, the Fritzing simulator version 1.0.4 was used, allowing verification of connection integrity before physical implementation. Raw data processing, tabulation of field tests, and generation of descriptive charts were performed in Microsoft Excel 2021. Finally, for sample size calculation and inferential statistical analysis of percentage errors, Minitab® version 21.4 was used, configured for a 95% confidence level.

2.5. Data Collection Procedures

Data collection was structured in two main phases.

2.5.1. Pre-Intervention Phase

For the tested 2012 Hyundai Accent, the maintenance thresholds programmed into the prototype were taken from the corresponding Hyundai owner's manual as follows: engine oil and filter, 12,000 km or 6 months; brake-related inspection items, including brake hoses/lines and front/rear brake components, from 24,000 km or 12 months onward; brake/clutch fluid inspection, 48,000 km or 24 months; manual transaxle fluid inspection (if equipped), 60,000 km or 30 months; and iridium spark-plug replacement, 168,000 km or 84 months. These values were extracted from the scheduled maintenance service section of the Hyundai Accent (2012) Owner's Manual [25].

2.5.2. Post-Intervention Phase

Once the prototype was installed in the vehicle (see physical assembly in Figures A2–A5), the system automatically began calculating the distance traveled from GPS coordinates. The vehicle odometer reading was manually recorded at the start and end of each weekly test period, enabling direct comparison with the GPS Ublox Neo 6M module measurement. Each alert event generated was automatically logged to the MicroSD card, including the date, time, remaining mileage for each maintenance interval, and total mileage.

Laboratory tests included verification of GPS signal reception, reliability of SMS alert sending using the A7670SA GSM module, and measurement of system latency. Only after meeting the established technical criteria were field tests conducted under real operating conditions.

2.6. Maintenance Alert Algorithm

The implemented algorithm continuously compares the accumulated mileage calculated by the GPS module against the maintenance thresholds defined for each vehicle. When proximity to a maintenance interval is detected, the system generates three progressive SMS alerts: a first alert at 50 km before the scheduled maintenance, a second at 10 km, and a third upon reaching the exact established mileage. This strategy enables anticipatory planning of maintenance interventions.

The three-level alert distances adopted in this prototype (50 km, 10 km, and 0 km) were defined as a practical engineering heuristic intended to provide graduated warning urgency before the scheduled maintenance point. These thresholds were not derived from a dedicated user-behavior study and should therefore be interpreted as an initial fixed policy rather than as an empirically optimized alert schedule. A complete overview of the firmware architecture, including the configuration logic, GPS-based odometry, alert generation, and state persistence, is provided in Listing A1 in Appendix D.

2.7. Data Analysis Methods

Data analysis was developed using descriptive statistical techniques. GPS system performance was quantified by calculating the Mean Absolute Percentage Error (MAPE)

and the Root Mean Square Error (RMSE) relative to the vehicle odometer record as the operational reference used for maintenance scheduling. Accordingly, these indicators should be interpreted as agreement metrics with respect to the dashboard mileage reading, rather than as absolute accuracy against an independently calibrated geodetic standard. Detailed results of these indicators are presented in Table A3.

The performance of the alert system was evaluated using a confusion matrix, in which events were categorized as correct and incorrect detections, both positive and negative [26]. From this classification, the overall precision index of the system was calculated, considering values above 95% as valid.

Finally, system latency was analyzed through descriptive statistics, estimating the mean and standard deviation of the time elapsed between the activation of the maintenance threshold and the user's receipt of the SMS (see statistical summary in Table A4). The system met the requirements when the latency was below 10 s.

2.8. Statistical Determination of Sample Size

To ensure the representativeness of the experimental data, an initial pilot phase was conducted consisting of 3 repetitions for each test scenario. From these preliminary results, the standard deviation of the measurement error (S) was calculated for each route type.

To ensure the accuracy of the final results, Minitab statistical software was used to determine the minimum sample size (n) required to estimate the mean error with a 95% confidence level ($Z = 1.96$). Maximum permissible error margins (E) specific to each distance scale were established, yielding the following experimental design parameters:

Urban Route (A): An initial standard deviation of $S = 0.065$ km was observed. For a target error margin of 0.1, the calculation determined a sample size of 5 repetitions. **Peripheral Route (B):** With a pilot standard deviation of $S = 0.161$ km and an admissible error margin of 0.2, 5 repetitions were required.

Long-Distance Route (C): Due to higher variability in route conditions (error standard deviation $S = 0.709$ km), an error margin of 0.5 was set, yielding a requirement of 11 repetitions.

3. Results

The results of the validation are presented below.

3.1. Experimental Validation of the Proposed System

To verify system functionality, specific tests were carried out on each of its main subsystems that support the prototype's functionality: positioning (GPS), communication (LTE/GSM), storage (MicroSD), and energy/ignition state (voltage detection). The results are organized by subsystem, including the measured parameters, observed behavior, and the corresponding technical interpretation.

3.1.1. Validation of the Global Positioning Module (GPS)

GPS module validation aimed to verify three essential aspects for prototype operation: (i) the ability to acquire a satellite signal in an adequate time (Fix), (ii) the accuracy of the calculated distance traveled via coordinate-based odometry, and (iii) the consistency of the accumulated error when compared to the vehicle odometer, used as the operational field reference.

The 3.0 km/h filtering threshold was selected as a low-speed cutoff to reduce phantom accumulation associated with GPS drift during stop-and-go operation. This choice is consistent with the broader observation that congested urban traffic exhibits highly variable speed behavior and complex low-speed dynamics, which complicate speed-related modeling and interpretation in dense urban environments. However, the threshold should

be understood as a context-dependent design choice for the present prototype and not as a universally optimal boundary [19].

Signal Acquisition Time (Fix).

In the static cold-start test, the GPS module achieved a valid satellite fix in an average time of 45 s. This result is considered adequate for an embedded system operating with consumer-grade GNSS signals, especially considering that in real scenarios, the initial fix is often affected by environmental conditions (partial obstruction, satellite availability, and signal quality). The recorded time allows the system to be operational within a reasonable interval from vehicle start-up, enabling the initiation of distance counting and maintenance logic without prolonged delays.

Accuracy of Accumulated Distance Measurement.

The prototype's odometry is based on the accumulation of distances between successive points calculated from the GNSS coordinates. To reduce the impact of "urban noise" and avoid accumulation of micro-displacements when the vehicle is stationary (e.g., at traffic lights), firmware logical filtering was applied. Distance calculation was optimized using the native function of the TinyGPS++ library (`distanceBetween`), replacing complex manual calculations. Additionally, firmware logic was applied to discard displacements at speeds below 3.0 km/h or distances less than 5 m between readings. This approach reduces the risk of "phantom sums" in stop-and-go environments.

The following code as shown in Listing 1 excerpt illustrates how the algorithm calculates real distance and dynamically updates maintenance counters:

Listing 1. GPS processing and odometer update logic executed in the main loop.

```
// GPS processing logic and odometer update (inside void loop)
while (Serial1.available() > 0) {
  if (gps.encode(Serial1.read())) {
    if (engineOn && isConfigured) {
      if (gps.location.isValid()) {
        if (firstFix) {
          lastLat = gps.location.lat();
          lastLon = gps.location.lng();
          firstFix = false;
        } else {
          double distMeters = gps.distanceBetween(
            gps.location.lat(), gps.location.lng(),
            lastLat, lastLon);

          // Urban noise filters (Stop-and-Go)
          if (gps.speed.kmph() > 3.0 && distMeters > 5.0) {
            totalOdometer += (unsigned long)distMeters;

            // Dynamic update of 6 maintenance counters
            for (int i = 0; i < NUM_MAINT; i++) {
              maintCounters[i] += (unsigned long)distMeters;
            }

            lastLat = gps.location.lat();
            lastLon = gps.location.lng();
          }
        }
      }
    }
  }
}
```

It should be noted that accepted GPS segments are accumulated at integer-meter resolution, since the floating-point value `distMeters` is cast to `unsigned long` before storage in `totalOdometer` and `maintCounters`. This introduces a sub-meter quantization of each accepted increment; however, its effect is considered negligible relative to the route-level disagreement observed in the present experiments, which was dominated by errors on the order of hundreds of meters to kilometers rather than by meter-level discretization.

GPS vs. Vehicle Odometer Comparison.

The dynamic test consisted of a controlled long-distance trip, using the vehicle's digital odometer as a practical reference. After completing a standard route of 160.0 km (odometer), the prototype recorded 164.0 km as accumulated distance. In relative terms, this difference represents an error of approximately +2.5%, evidencing a positive deviation (overestimation). The relationship between both measurements is expressed by Equations (1) and (2):

$$E_{\text{abs}} = |V_{\text{ref}} - V_{\text{meas}}| = |160.0 - 164.0| = 4.0 \text{ km} \quad (1)$$

$$E_{\text{rel}} = \frac{E_{\text{abs}}}{V_{\text{ref}}} \times 100 = \frac{4.0}{160.0} \times 100 = 2.5\% \quad (2)$$

where E_{abs} is the absolute error, E_{rel} is the relative error, V_{ref} is the odometer-based reference value, and V_{meas} is the prototype measurement.

Error Margin Analysis and Systematic Tendency.

The 2.5% error observed in the 160.0 km trip is satisfactory as a characterization of cumulative odometric drift over an extended route. However, this test does not isolate stationary or very-low-speed phantom-distance accumulation, which is one of the main error sources in dense urban stop-and-go traffic. Therefore, the discrepancy between the dense urban and peripheral scenarios should be interpreted together with the route-level results, where the higher urban MAPE is consistent with residual multipath and stop-and-go drift despite the implemented 3.0 km/h and 5 m thresholds. A dedicated static or low-speed creeping test was not included in the present experimental campaign and is identified as a priority for future validation of the filtering strategy.

3.1.2. Validation of the LTE/GSM Communication Module

The communication subsystem validation aimed to guarantee the prototype's ability to operate on the current telecommunications infrastructure, prioritizing fast connectivity, link stability, and low latency in alert delivery. Unlike traditional 2G solutions, the module used (A7670SA) allows LTE network operation, which improves the performance in environments where 2G coverage is limited or obsolete.

SMS Alert Transmission Latency.

System latency was evaluated through 20 consecutive alert transmissions under standard coverage conditions. The detailed transmission times are reported in Table A4, from which a mean latency of 4.13 s, a standard deviation of 0.63 s, and a maximum recorded value of 5.00 s were obtained. Complementarily, Table 1 summarizes the observed outcomes of these controlled triggered alert-transmission tests, confirming that all 20 triggered alerts were successfully delivered under the tested conditions. Taken together, these results validate compliance with the design requirement (<10 s), aligning with delivery times reported in the literature for low-cost SMS-based telemetry systems [27,28].

To evaluate the alert-delivery reliability, 20 controlled triggered alert transmissions were generated under standard coverage conditions for subsystem validation. These events should be interpreted as directed test activations rather than as organically occurring long-term field events. Because the present validation did not systematically sample below-

threshold negative cases, a full confusion-matrix framing is not appropriate, and metrics such as true negatives, specificity, and false-positive rate were not estimated in this study.

Table 1. Observed outcomes of controlled triggered alert-transmission tests under standard coverage conditions.

Outcome	Count
Triggered alert successfully delivered	20
Triggered alert not delivered	0

Under the tested conditions, the observed alert-delivery success proportion was 20/20 = 100%. The corresponding exact 95% binomial confidence interval for the success probability was 83.2–100.0%. Expressed in complementary form, the equivalent exact 95% interval for the failure probability was 0.0–16.8%. Therefore, although no delivery failures were observed in the controlled tests, these results should not be interpreted as proof of long-term field reliability.

Figure 2 shows the SMS alert message as received on the vehicle owner's mobile device, confirming the end-to-end communication chain from the prototype to the user.

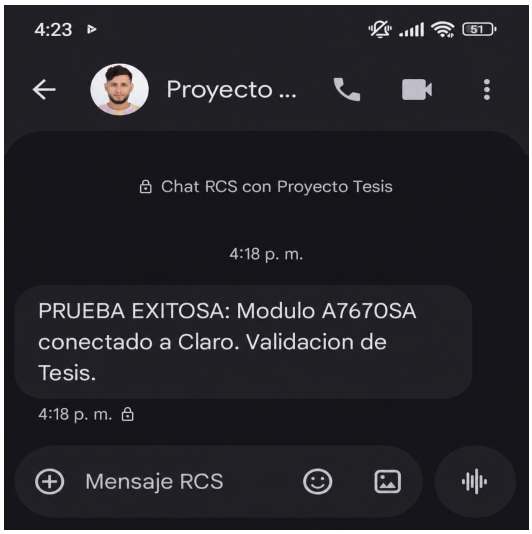

Figure 2. SMS maintenance alert received on the owner's mobile device.

3.1.3. Validation of the Data Storage System

The storage module (MicroSD) fulfills a critical function by supporting information persistence across power cycles and enabling the historical logging of mileage, events, and alerts. Its validation focused on correct hardware initialization, the implemented write/recovery behavior, and the ability to restore state after the tested power interruptions.

The storage system was redesigned to fulfill a dual critical function: hosting a static database (`DATA.CSV`) with the profiles and specific maintenance schedules for various vehicle models and retaining the user's dynamic configuration in a local file (`CONFIG.TXT`). The latter stores the owner's contact number, selected vehicle, total odometer, and real-time counters for up to six independent maintenance intervals.

As shown in the code excerpts (see Listing 2), the implemented file-management strategy is intentionally simple. DATA.CSV is used as a static lookup table and is not modified during operation, while CONFIG.TXT stores only the dynamic state. When state persistence is triggered, the firmware removes the previous CONFIG.TXT file, rewrites the full state sequentially, and closes the file immediately after completion. During startup, the loader first verifies the file existence and then performs basic structural validation

by checking the expected comma delimiters before accepting each maintenance record. The current prototype does not implement temporary files, mirrored backups, or checksum/CRC verification. Therefore, although successful state recovery was observed after the tested power interruptions, an interruption occurring during the brief rewrite window could still leave CONFIG.TXT incomplete. Future iterations will incorporate transactional commit and integrity-verification mechanisms to reduce this residual risk.

Listing 2. Functions for saving and loading user configuration and maintenance data.

```
// User configuration and maintenance persistence functions
void saveConfig() {
  SD.remove("CONFIG.TXT");
  File file = SD.open("CONFIG.TXT", FILE_WRITE);
  if (file) {
    file.println(ownerNumber);
    file.println(currentYear);
    file.println(currentModel);
    file.println(totalOdometer);
    for (int i = 0; i < NUM_MAINT; i++) {
      file.print(maintNames[i]); file.print(",");
      file.print(maintIntervals[i]); file.print(",");
      file.println(maintCounters[i]);
    }
    file.close();
  }
}

bool loadConfig() {
  if (!SD.exists("CONFIG.TXT")) return false;
  File file = SD.open("CONFIG.TXT");
  if (file) {
    ownerNumber = file.readStringUntil('\n'); ownerNumber.trim();
    currentYear = file.readStringUntil('\n'); currentYear.trim();
    currentModel = file.readStringUntil('\n'); currentModel.trim();
    String odoStr = file.readStringUntil('\n'); odoStr.trim();
    totalOdometer = odoStr.toInt();
    for (int i = 0; i < NUM_MAINT; i++) {
      String line = file.readStringUntil('\n');
      int firstComma = line.indexOf(',');
      int secondComma = line.lastIndexOf(',');
      if (firstComma > 0 && secondComma > firstComma) {
        maintNames[i] = line.substring(0, firstComma);
        maintIntervals[i] =
          line.substring(firstComma+1, secondComma).toInt();
        maintCounters[i] =
          line.substring(secondComma+1).toInt();
        alert50[i]=false; alert10[i]=false; alert0[i]=false;
      }
    }
    file.close();
    return true;
  }
  return false;
}
```

System State Recovery.

After restoring power, the system executed the recovery routine from the stored state file and successfully restored the last valid saved mileage in the tested power-cycle scenarios. This behavior supports operational continuity for the evaluated interruptions, but it should not be interpreted as a fully fault-tolerant guarantee against power loss during an active write cycle.

3.1.4. Validation of the Energy and Virtual Ignition System

The power system was validated with two objectives: (i) to ensure that the electronics operate under stable conditions against typical automotive electrical system variations and (ii) to verify the effectiveness of the voltage-based "virtual ignition" algorithm, avoiding the need for physical connection to the ACC wire and enabling direct connection to the battery terminals (Figure A4).

Power Supply Stability.

During tests, the voltage regulator maintained a stable 5 V output for inputs up to 14.5 V, a range consistent with automotive operation when the alternator is under load. This result indicates that the regulation stage is adequate for protecting the microcontroller and associated modules against fluctuations in the vehicle's electrical system.

Engine State Detection by Voltage.

The virtual ignition algorithm correctly discriminated engine states by reading the battery voltage using a conversion factor adjusted to 5.7. Clearly differentiated ranges were established to avoid erratic states:

- Engine off: (<12.9 V) → system in standby mode (no distance accumulation).
- Engine on: (>13.8 V) → system in active mode (km counting and threshold evaluation enabled).

This logic is implemented as a virtual ignition strategy, as shown in Listing 3.

Listing 3. Engine-state detection based on battery voltage thresholds (virtual ignition).

```
// Engine state detection function (Virtual ignition)
void readVoltage() {
  // Conversion factor 5.7 for the implemented voltage divider
  int adc = analogRead(PIN_VOLT);
  batteryVoltage = (adc * 5.0 / 1023.0) * 5.7;

  if (batteryVoltage > 13.8) {
    engineOn = true;
  } else if (batteryVoltage < 12.9) {
    engineOn = false;
  }
}
```

3.2. Field Test Results on Real Routes

To evaluate the system performance under real operating conditions, field tests were conducted based on the repetition of representative trajectories (illustrated in Figure A3) for the most frequent driving scenarios: dense urban environment, mixed peripheral road, and long-distance routes. In each case, the distance traveled calculated by the prototype was directly compared against the vehicle's odometer reading, considered the operational reference. The obtained results are presented below.

3.2.1. Results on Dense Urban Route

Urban route tests were performed in an environment characterized by heavy traffic, multiple traffic lights, and frequent stops—conditions representing the most demanding scenario for satellite positioning systems, due to the urban canyon effect and signal drift in stop-and-go situations.

Route A was defined within the urban center of Guayaquil, characterized by high vehicle flow and frequent traffic lights. The route begins in the south of Guayaquil, departing from the Cangrejo Fútbol sportsbar, and advances northward along Avenida Quito, crossing a large part of the city to the center, where an intermediate stop is made at Picantería "El Sargento Mayor." For the return, the route descends southward again, first

taking Lorenzo de Garaycoa street, then turning onto Vicente Trujillo street, and finally onto Av. Domingo Comin to conclude near the Guayas riverbank, specifically at the Caraguay Market Metrovía stop, as illustrated in Figure 3. The route-level results for the dense urban scenario are summarized in Table 2.

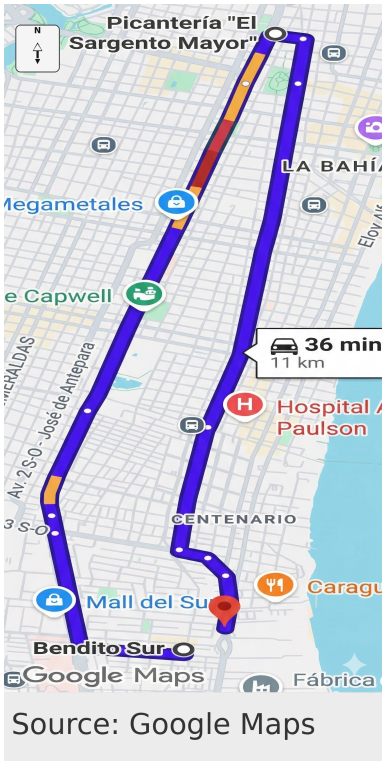

Figure 3. Route A: Dense urban route in Guayaquil city center. Source: Google Maps web interface (accessed on 1 December 2025).

Table 2. Results: Route A (dense urban—11.0 km).

Repetition	Real Distance (Odometer)	Prototype Distance	Deviation (km)	Error (%)
Test A-1	11.00 km	11.67 km	+0.67 km	6.09%
Test A-2	11.00 km	11.76 km	+0.76 km	6.91%
Test A-3	11.00 km	11.69 km	+0.69 km	6.27%
Test A-4	11.00 km	11.73 km	+0.73 km	6.64%
Test A-5	11.00 km	11.70 km	+0.70 km	6.36%
AVERAGE	11.00 km	11.71 km	+0.71 km	6.45%

The average percentage error was 6.45% (overestimation). This deviation is the highest of the three scenarios and is attributed to the "multipath" effect or signal reflection off tall buildings in the city center. This phenomenon introduces "noise" into GPS coordinates, adding phantom extra meters while the vehicle moves slowly or is stopped at traffic lights, generating a count higher than the real distance. The higher urban-route error is consistent with the limits of the implemented rule-based filter. Although the speed and minimum-segment thresholds suppress a substantial portion of low-speed drift, they do not completely eliminate multipath-induced coordinate jitter in dense urban canyons. This explains why the dense urban route remained the most demanding scenario for the prototype.

It should also be noted that this urban-route MAPE of 6.45% exceeds the 4% benchmark adopted in this study as a practical control limit. Therefore, under dense urban conditions, the present prototype cannot be considered compliant with that reference criterion.

3.2.2. Results on Mixed Peripheral Route

The mixed peripheral route corresponds to an intermediate scenario, characterized by moderate speeds (40–60 km/h), fewer stops, and continuous-flow sections. This environment enables the evaluation of system behavior when the GPS operates with more stability and less urban interference.

Route B begins in the southern part of the city, at Persianas Ecuador, and heads northward through Guayaquil primarily via the Vía Perimetral. The route continues to the reference point at Maximetales S.A. Norte, located in the northern sector of the city. From this point, the route returns following the same road axis back to the origin, completing a total round trip of 41 km south–north–south, as shown in Figure 4. The route-level results for the mixed peripheral scenario are summarized in Table 3.

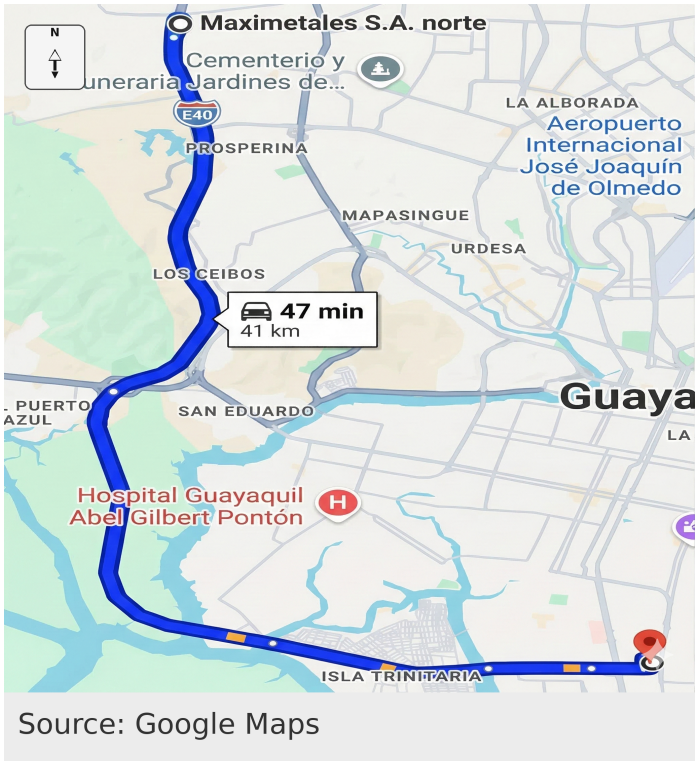

Figure 4. Route B: Mixed peripheral route via Vía Perimetral. Source: Google Maps web interface (accessed on 1 December 2025).

Table 3. Results: Route B (mixed peripheral—41.0 km).

Repetition	Real Distance (Odometer)	Prototype Distance	Deviation (km)	Error (%)
Test B-1	41.00 km	41.87 km	+0.87 km	2.12%
Test B-2	41.00 km	41.82 km	+0.82 km	2.00%
Test B-3	41.00 km	41.86 km	+0.86 km	2.10%
Test B-4	41.00 km	41.88 km	+0.88 km	2.15%
Test B-5	41.00 km	41.84 km	+0.84 km	2.05%
AVERAGE	41.00 km	41.85 km	+0.85 km	2.08%

The results show an average error of 2.08%. The significant reduction in error compared to the urban route (6.45%) confirms that, as the building density decreases, and the average speed increases, the system improves its precision, while maintaining a slight positive tendency.

3.2.3. Results on Interurban Routes

Tests in the interurban scenario were carried out on a controlled 32 km route, designed to evaluate behavior at constant cruising speed. The obtained results (Table 4) show an average deviation of +1.09 km, representing a mean error of 3.40%.

Unlike the peripheral route (where the error was lower, 2.08%), in this scenario, the sustained constant speed appears to have influenced the systematic accumulation of positive micro-positioning errors. This confirms a consistent tendency of the module to slightly overestimate distances on continuous routes without stops, aligning with the expected positive bias.

Route C begins on the Vía a la Costa highway, at the Delportal supermarket, continues along this main artery to the Chongón entrance (the return point), and finishes at the same starting location, forming a round trip of 32 km, as shown in Figure 5.



Figure 5. Route C: Interurban route on Vía a la Costa. Source: Google Maps web interface (accessed on 1 December 2025).

Table 4. Results: Route C (interurban road).

Repetition	Real Distance (Odometer)	Prototype Distance	Deviation (km)	Error (%)
Test C-1	32.00 km	33.06 km	+1.06 km	3.31%
Test C-2	32.00 km	33.10 km	+1.10 km	3.44%
Test C-3	32.00 km	33.09 km	+1.09 km	3.41%
Test C-4	32.00 km	33.08 km	+1.08 km	3.37%
Test C-5	32.00 km	33.09 km	+1.09 km	3.42%
Test C-6	32.00 km	33.11 km	+1.11 km	3.47%
Test C-7	32.00 km	33.08 km	+1.08 km	3.36%
Test C-8	32.00 km	33.08 km	+1.08 km	3.36%
Test C-9	32.00 km	33.11 km	+1.11 km	3.47%
Test C-10	32.00 km	33.10 km	+1.10 km	3.42%
Test C-11	32.00 km	33.07 km	+1.07 km	3.35%
AVERAGE	32.00 km	33.09 km	+1.09 km	3.40%

The low dispersion observed confirms that the error does not grow in an uncontrolled manner with increasing distance, but it maintains stable proportionality relative to the total distance traveled. This behavior is indicative of a systematic and predictable drift, characteristic of commercial-grade GNSS systems without differential correction.

From an operational standpoint, this consistency is especially relevant, as it allows anticipation of system behavior on extensive routes and validates its use for mileage-based preventive maintenance management.

3.3. Statistical Analysis of Results

3.3.1. Analysis of Accumulated Percentage Error

The consolidation of results reveals a clear pattern: the system overestimates distance in all scenarios. The mean error was 6.45% in urban, 2.08% in peripheral, and 3.40% in interurban routes. The global mean error of the system stands at **3.98%**. This consistency in overestimation (Positive Bias) is fundamental for reliability, as it indicates that the error is not random but systematic and predictable.

However, the global mean of 3.98% should not be interpreted as uniform compliance across all scenarios, since the dense urban route remained above the 4% benchmark, while the peripheral and interurban routes remained below it.

In the current prototype, GPS noise mitigation was implemented as a deterministic rule-based filter rather than as a Kalman-based estimator. After the first valid GPS fix initializes the reference coordinates, the firmware computes the distance between consecutive valid coordinates using the TinyGPS++ `distanceBetween()` function. Distance accumulation is enabled only when the system is configured, and the virtual ignition state is active. Candidate increments are discarded when the reported speed is below 3.0 km/h or when the segment length between consecutive samples is below 5 m, since such increments are typically associated with stop-and-go drift and multipath-induced phantom distances near traffic lights. No HDoP-based rejection criterion was implemented in the current version.

3.3.2. Comparison Between Satellite and Mechanical Odometry

The discrepancy observed between the odometry calculated by the prototype and the vehicle odometer reading responds to inherent differences between both measurement methods. While the satellite system calculates the distance by summing geodetic segments between discrete positions, the mechanical odometer is based on tire rotation, being sensitive to physical factors such as inflation pressure and wear.

In this context, a systematic positive error close to 2.5% falls within the acceptable margins for consumer-grade GNSS instrumentation. From a maintenance engineering perspective, this behavior is even favorable, as it introduces a quantifiable operational safety margin: projecting the mean error over a typical 5000 km maintenance cycle, the system will generate the alert at approximately 4875 real km, anticipating the intervention and reducing to zero the risk of exceeding the critical component operation limit.

3.3.3. Statistical Validation of Mean Differences

To determine whether the observed difference between the prototype measurement and the vehicle odometer is statistically significant, an inferential analysis was conducted using Minitab software, applied independently for the three test scenarios (Urban, Peripheral, and Interurban routes).

First, the normality assumption was verified using the Shapiro–Wilk test. In all three evaluated scenarios, p-values > 0.100 were obtained, indicating that the data follow a normal distribution and confirming that the data distribution is parametric. The corresponding normal probability charts are presented in (Figures A6–A8).

Because the prototype and the vehicle odometer represent two measurement methods applied to the same trips, method agreement was assessed using a route-specific Bland–Altman analysis rather than relying only on hypothesis testing. For each route type, the paired difference was defined as Prototype minus Odometer and plotted against the mean of both methods. The mean bias and the 95% limits of agreement, computed as the mean

difference plus and minus 1.96 standard deviations, are summarized in Table A5, while the corresponding plots are presented in Figures A9–A11.

The Bland–Altman analysis confirmed a consistent positive bias in all scenarios. For the dense urban route, the mean bias was +0.710 km, with 95% limits of agreement from +0.641 to +0.779 km. For the mixed peripheral route, the mean bias was +0.854 km, with limits from +0.807 to +0.901 km. For the interurban route, the mean bias was +1.088 km, with limits from +1.057 to +1.120 km. In all three cases, the limits of agreement remained entirely above zero, indicating systematic overestimation rather than random bidirectional disagreement between methods under the tested conditions.

From an engineering perspective, this result is relevant because it shows that the disagreement between the prototype and the odometer remained bounded and conservative within each tested scenario. Therefore, the proposed alert logic operates with a predictable anticipatory margin, which is preferable to delayed notification in preventive-maintenance applications.

3.4. Discussion of Results and Experimental Conclusions

The comprehensive evaluation of the proposed system, based on unit and field tests conducted, allows analysis not only of the quantitative performance of each subsystem but also of the overall reliability of the prototype as a support tool for preventive vehicle maintenance management. The results obtained provide evidence of coherent, stable, and technically consistent behavior, adequate for application in light vehicles under real operating conditions.

3.4.1. Consistency and System Reliability

One of the most relevant findings of the study is the measurement system's consistency, observed across different route typologies and operating conditions. The filtering logic implemented in the GPS module was intended to mitigate urban noise and reduce the accumulation of micro-displacements when the vehicle is stationary. In demanding scenarios such as dense urban traffic, the system still exhibited bounded and repeatable error; however, because no dedicated stationary or creeping drift protocol was performed, the effectiveness of the filtering strategy should be interpreted from the route-level error pattern rather than as a direct experimental quantification of phantom-distance suppression.

Repetition of trajectories under similar conditions allowed verification of the measurement repeatability, evidenced by the low dispersion of percentage error between consecutive tests. In particular, in long-distance routes, the error variation remained within a narrow range, indicating that the observed deviation is not the product of random fluctuations but of systematic behavior inherent to the satellite measurement method. This characteristic is essential for preventive maintenance applications, where system predictability is a key factor for reliable decision-making.

Taken together, these results validate that the system is not only functional but also reliable over time, preserving its performance under different traffic conditions, speeds, and environments, meeting the technical criteria defined in the methodological phase.

3.4.2. System Operational Safety Margin

Analysis of the impact of the measurement error on maintenance cycles allows evaluation of the system from an operational and reliability engineering perspective. The observed systematic positive error, with a mean value close to 2.5%, implies that the system tends to slightly overestimate the distance traveled. Projecting this behavior over a typical 5000 km maintenance cycle, the alert would be generated at approximately 4875 real km, introducing an anticipation margin of approximately 125 km. Consistent with this interpretation, the Bland–Altman upper limits of agreement also remained positive in all scenarios

(+0.779 km urban, +0.901 km peripheral, and +1.120 km interurban), indicating that the prototype maintained a bounded conservative overestimation under the tested conditions.

This behavior adheres to the "fail-safe" design principle, widely applied in critical-systems, where safety is prioritized over absolute precision. In the context of vehicular maintenance, it is preferable for the system to anticipate the need for intervention before the component reaches its critical operating limit, rather than delaying the alert and increasing the risk of excessive wear or mechanical failure.

From this perspective, the observed operational safety margin does not represent a limitation of the system, but a functional advantage, as it protects engine and component integrity regardless of driving style or road conditions. Experimental results consequently confirm that the proposed system fulfills its fundamental objective: optimizing preventive maintenance management through timely, reliable, and safety-oriented alerts.

4. Discussion

4.1. Analysis of Technical Precision Against Industry Standards

The experimental results yielded a global systematic mean error of 3.98% (overestimation) in distance measurement. Contrasting this value with the specialized literature, consistent behavior is evident across all three evaluated scenarios, where the deviation was invariably positive, validating the "Positive Bias" theory [29]. This phenomenon, inherent to the discrete sampling of trajectories via GPS in environments with signal noise, mathematically explains the tendency observed in our tests. In this context, the recent literature agrees that experimental evaluation of systems applied to the vehicular environment should be conducted under real operating conditions, as these more accurately reflect the technical challenges associated with urban traffic and vehicle–infrastructure interaction [30].

Despite variations by environment, the overall prototype performance remains within the accepted safety ranges. As a regulatory reference, the National Institute of Standards and Technology (NIST) establishes a 4% acceptance tolerance for vehicle odometers [18]. Given that the observed global mean deviation relative to the dashboard odometer was 3.98%, the overall disagreement remained close to the 4% benchmark used in this study as a practical engineering reference. However, this overall value must be interpreted together with the route-specific results, since the dense urban scenario exceeded that benchmark with a MAPE of 6.45%, whereas the peripheral and interurban scenarios remained below it.

Finally, in terms of road safety, the automation of alerts reduces dependence on driver memory, mitigating the risk of accidents caused by mechanical failures, which are consistently reported by ANT [31]. Similarly, compliance with maintenance intervals favors control of pollutant emissions (CO, CO_2, NO_x), aligning with the objectives of current environmental regulations [5,6].

4.2. Economic Impact and Viability in Maintenance Management

The viability of an aftermarket telemetry system depends directly on its economic accessibility compared to existing market alternatives. To evaluate this aspect, a comparative analysis was performed between the proposed prototype and two widely distributed commercial solutions (Vyncs and Fleetio), detailed in Table 5.

Table 5. Comparison of similar solutions.

Solution	Technology	Initial Cost	Monthly Cost	Communication	Limitations
Vyncs	OBD-II tracker with DTC reader	$146	$22.00	Proprietary app (internet)	Depends on data coverage; manual scheduling
Fleetio	Fleet management cloud software	N/A	$10.00	Proprietary app (internet)	Limited automated integration; requires daily manual km update
Proposed Prototype	Satellite telemetry-based preventive alert system	$78.84	$3.00 (SMS)	SMS messaging	Does not extract DTC fault codes from ECU

N/A = not applicable, since Fleetio is a cloud-based software service and no dedicated initial hardware purchase was considered in the comparison presented.

Therefore, Table 5 should be interpreted as a contextual comparison of cost structure and deployment style, rather than as a direct comparison between functionally equivalent products.

4.2.1. Cost Structure and Scalability

The initial cost of $78.84 USD for the functional prototype represents the version built with standard commercial components (Arduino Mega, independent GPS/GSM modules) acquired at retail prices. A formal scalability analysis reveals significant optimization opportunities if the system advances to a manufacturing phase:

- **Series production (batches of 100 units):** Bulk component acquisition enables an estimated 25–30% cost reduction, placing the base cost between $55.00 and $59.00 USD. Migration toward a custom Printed Circuit Board (PCB) design would add approximately $15.00 USD per unit at this volume, resulting in a final production cost of ∼$70.00–$74.00 USD per device.
- **Industrial production (batches of 1,000+ units):** Scaling production and integrating Surface Mount Device (SMD) components directly into a System-on-Chip (SoC) design reduces manufacturing costs by 40–45%. The projected cost would drop to ∼$43.00–$47.00 USD per unit, also achieving higher physical robustness and a significantly smaller installation size.

4.2.2. Illustrative Economic Scenario for Potential End-User Adoption

To provide an initial economic perspective, an illustrative implementation scenario was considered using a projected retail price of $120.00 USD and a monthly operating cost of $3.00 USD for basic SMS service. Under these assumptions, the first-year total cost of ownership (TCO) of the proposed prototype would be $156.00 USD. For broad market context, this value was contrasted with selected commercial references such as Vyncs; however, this comparison should not be interpreted as a feature-equivalent benchmark, since commercial OBD-II ecosystems may include additional functions such as DTC reading, app integration, and cloud services that are outside the current scope of the present prototype [4].

Considering that 75% of the Ecuadorian vehicle fleet exceeds 6 years of age and lacks native telematics systems [2], this solution demonstrates not only economic viability but also structural relevance for mitigating the high operating costs of the sector. Likewise,

the maintenance-cost scenario used to illustrate the possible economic benefit should be interpreted cautiously. The annual preventive-maintenance expenditure assumed in this subsection is not intended as a universally representative value for all private light-vehicle owners, whose mobility patterns and service costs may vary substantially. For this reason, the resulting savings and payback figures should be understood as scenario-based projections rather than as validated ROI estimates for the broader private-vehicle market.

This caution is especially relevant because private vehicle users do not constitute a homogeneous operational group: commute distance, mode choice, and daily mobility intensity can vary substantially across users and urban contexts [32].

4.3. Impact on Maintenance Management

Beyond economic viability, the experimental results provide preliminary engineering evidence of how the proposed system can support preventive-maintenance management through timely alert generation and an anticipatory operating margin. However, these findings should not be interpreted as a direct demonstration of real-world maintenance-compliance improvement, since the experimental window was not long enough to observe organic maintenance-interval crossings or sustained user response behavior. In this study, the pre/post comparison is therefore limited to the contrast between manual mileage dependence and the technical operation of the automated alert prototype under the tested conditions [3]; after implementation, the system achieved successful delivery in 20 out of 20 controlled triggered alert tests under the tested conditions, corresponding to an observed success proportion of 100% and an exact 95% binomial confidence interval of 83.2–100.0%. However, because below-threshold negative cases were not systematically sampled, and no user-response behavior was directly observed, this result should be interpreted as evidence of triggered-alert delivery performance rather than as direct behavioral evidence of reduced omission associated with the "forgetfulness factor".

However, this result should be interpreted as a reduction in dependence on user memory under a fixed alert policy, rather than as a direct quantification or behavioral adaptation of the user's forgetfulness factor. The current prototype uses static warning thresholds and does not yet adjust its alert timing according to the driver's observed responsiveness.

Second, the systematic 2.5% positive bias introduces a quantifiable anticipation margin: projected over a typical 5000 km cycle, the system generates the alert at approximately 4875 real km, anticipating the critical threshold by 125 km and reducing to zero the risk of interval overshoot if the driver responds to the notification. This behavior is consistent with what has been documented in automatic alert systems for machinery, where alert automation has been shown to improve adherence to maintenance schedules and reduce unplanned downtime [13]. Together, these two indicators—100% notification effectiveness and deterministic 125 km anticipation per cycle—constitute quantitative evidence of compliance with the preventive maintenance optimization objective set out in this study.

4.4. Technical Comparison Against On-Board Diagnostic Systems (OBD-II)

It should also be noted that the commercial solutions included in Table 5 represent selected benchmarks and do not imply that all OBD-II-based ecosystems necessarily require a dedicated subscription or higher total cost in every user scenario.

While the recent literature proposes OBD-II-based monitoring solutions and cloud platforms for fleet management [7], this project opted for an independent hardware architecture. To objectively evaluate the differences between both solutions, a technical comparative analysis was developed (Table 6), contrasting the capabilities of the OBD-II standard against the proposed satellite system.

The comparison in Table 6 shows that the choice between both architectures is scenario-dependent rather than absolute. For vehicles with reliable OBD-II compatibility, and for users willing to rely on a smartphone application, OBD-II-based solutions may be preferable because they can provide direct ECU diagnostics, richer user interfaces, and potentially lower recurring communication costs when the phone supplies GPS and cellular connectivity. By contrast, the contribution of the present prototype lies in offering a standalone ECU-independent alternative for aging or compatibility-limited vehicles, particularly when non-intrusive deployment and autonomous SMS alerting are prioritized over diagnostic depth.

However, the present interpretation should be understood as evidence of technical feasibility in a representative aging light vehicle rather than as definitive proof of universal applicability across all vehicle makers, model years, and electrical architectures. Broader multi-vehicle validation will be required to fully confirm the generalizability of this deployment approach.

In the Ecuadorian context, where 75% of the vehicle fleet exceeds 6 years of age, and 60% has more than 11 years of use [2], relying exclusively on the OBD-II port can reduce practical deployment flexibility in some vehicles. Depending on manufacturer-specific protocols, port condition, and electrical configuration, certain older vehicles may present access or compatibility constraints for generic scanners and app-assisted OBD-II solutions.

Table 6. Balanced comparison between app-assisted OBD-II solutions and the proposed prototype.

Technical Aspect	App-Assisted OBD-II Solution	Proposed Prototype (GPS/GSM)
Primary information source	Direct ECU/OBD-II data; smartphone GPS may complement trip logging and location services	GPS odometry, voltage-based virtual ignition, local MicroSD storage, and GSM/SMS alerts
Diagnostic capability	High: DTC reading and live ECU parameters	Limited: no direct ECU fault-code extraction
Connectivity path	Often Bluetooth to smartphone app; may use the phone's data plan and avoid a dedicated SIM card	Dedicated GSM/LTE module with SMS; standalone operation without smartphone
User interaction	Rich graphical interface and app notifications, but dependent on phone pairing, app availability, and user interaction	Simple SMS alerts and local persistence; lower interface richness but minimal user interaction once installed
Vehicle dependency	Preferable in vehicles with reliable OBD-II compatibility and accessible diagnostic port	Preferable in vehicles where OBD-II compatibility is uncertain, restricted, or not desired
ECU/CAN dependence	Requires access through the diagnostic port and a supported protocol	Electrically isolated from the ECU/CAN network
Operating cost structure	May be favorable when the user already has a smartphone and mobile data plan	Predictable standalone communication cost through dedicated SMS service
Best-fit scenario	Newer or protocol-compliant vehicles, especially when ECU diagnostics and app-based interaction are priorities	Aging fleets, compatibility-limited vehicles, or users prioritizing autonomous alerts independent of smartphone and ECU

By not depending on the on-board computer (ECU) or the OBD-II standard, the proposed system offers a potentially broader deployment path for aging or compatibility-limited vehicles. However, this advantage should presently be interpreted as a proof-of-concept finding supported by a representative single-vehicle validation, pending broader confirmation across multiple vehicle makers, ages, and electrical architectures [9].

4.5. Study Limitations

While the overall accuracy was satisfactory, larger error dispersion was observed on dense urban routes (6.45%) compared to peripheral routes (2.08%). This is consistent with findings reported by Hussain et al. [7], regarding the challenges of the "urban canyon" effect in IoT systems. The current version of the prototype uses a computationally lightweight rule-based filter based on speed and minimum-segment thresholds, which reduces low-speed phantom accumulation but does not fully suppress coordinate jitter in dense urban corridors. In addition, no HDoP-based rejection criterion or Kalman-type estimator was implemented in the present version. Because raw unfiltered GPS trajectories were not stored as a separate experimental dataset, a direct retrospective quantification of the error reduction achieved by the filter could not be reported in this study. Future work will therefore include an ablation comparison between raw and filtered GPS accumulation, as well as the incorporation of HDoP-based gating or Kalman filtering to further improve the performance under dense urban conditions.

Accordingly, the current rule-based filter cannot yet guarantee compliance with the 4% benchmark in the most demanding urban-canyon scenario, and more aggressive mitigation strategies will be required before such compliance can be claimed for dense urban use.

The present validation did not include a dedicated stationary or low-speed creeping protocol to directly quantify phantom-distance accumulation while the vehicle was stopped or moving near the filter threshold; therefore, the effect of this phenomenon is inferred indirectly from the higher dense-urban error and from the known influence of multipath in stop-and-go conditions. It is pertinent to note that direct quantification of the behavioral impact of the system—such as the percentage reduction in mileage overshoot measured over a sample of real drivers over several months—would require a longitudinal study with a control group beyond the scope of this work. The quasi-experimental design adopted is appropriate for technical prototype validation, which constitutes the necessary precondition prior to any large-scale deployment. Evaluation of the impact on user maintenance behavior constitutes a natural line of future research.

Accordingly, maintenance-compliance effectiveness in real users remains undemonstrated in the present study and will require longitudinal validation over longer operating periods, ideally with direct observation of actual maintenance actions after warning events. Moreover, although tire pressure was controlled to reduce one important source of odometer variation, no independent metrological verification of the odometer was performed. Therefore, any residual odometer error propagates directly into the reported MAPE and RMSE values as unquantified measurement uncertainty.

Although no alert-delivery failures were observed during the 20 tested events, larger-scale deployment could still be affected by factors not exhaustively evaluated in this study, such as temporary network instability, coverage transitions between cells, message delays, or other operational contingencies. Likewise, although the storage subsystem operated during the conducted vehicle-route tests, the present study did not include a dedicated accelerated vibration-endurance protocol of the MicroSD interface. Although the study is motivated by the practical consequences of the user's "forgetfulness factor", the current three-level alert strategy (50 km, 10 km, and 0 km) is statically defined and does not yet quantify or adapt to the user's actual response lag between the first warning and the subsequent maintenance action. Experimental validation was conducted on a single representative vehicle (2012 Hyundai Accent); so, the current results should be interpreted as strong evidence of technical feasibility rather than as a complete confirmation of universal applicability across the diversity of vehicle brands, ages, and electrical architectures present in real fleets.

In particular, parameters such as voltage-based ignition thresholds, GPS-related error behavior, and SMS delivery performance may vary across vehicles with different electrical conditions, installation layouts, and operating environments and therefore require explicit cross-vehicle validation before broader generalization. Likewise, the current communication validation did not include systematic sampling of below-threshold negative cases or long-term field monitoring beyond 20 controlled triggered alert tests; so, specificity, false-positive behavior, and extended reliability remain to be established in future work. In addition, the economic projections presented for end-user adoption were constructed as illustrative scenario-based estimates. A more robust ROI assessment will require maintenance-cost evidence specifically derived from private light-vehicle users and more direct market comparisons between functionally equivalent solutions.

Further, the three-tier alert distances were adopted as heuristic design values and were not optimized from user-response data, while the 3.0 km/h low-speed filtering threshold was not calibrated across multiple urban morphologies or congestion profiles. Both design parameters should therefore be interpreted as context-specific prototype settings requiring further validation in other operating environments.

5. Conclusions

This study demonstrates that the originality of the proposed system lies at the architecture and deployment level rather than at the component level. Its main contribution is the integration of filtered GPS odometry, voltage-based virtual ignition, configurable MicroSD-based persistence, and progressive SMS alert logic into an ECU-independent aftermarket solution for conventional light vehicles. Under the tested conditions, these results provide strong evidence of technical feasibility in a representative aging vehicle, supporting preventive-maintenance digitization through a non-intrusive and low-cost implementation.

Experimental validation evidenced distance measurement accuracy with a mean error of 3.98%, sufficient to guarantee the reliability of the established alert thresholds, as well as 100% effectiveness in SMS notification sending under the tested conditions (20/20 events; exact 95% binomial confidence interval: 83.2–100.0%). Additionally, an anticipation margin of approximately 2.5% relative to the 5000 km reference maintenance interval was obtained, which reduces the risk of exceeding critical service limits and favors the timely planning of interventions, while the average latency of 4.13 s confirmed its real-time operational capability. Together, these results support the feasibility of the proposed system as a practical engineering solution for more timely, controlled, and predictable preventive maintenance management.

The study concludes that the proposed technology is a viable solution to bridge the technological gap in the Ecuadorian vehicle fleet, whose average age exceeds 16 years. Accordingly, the proposed system should be interpreted as a complementary deployment path for aging or compatibility-limited vehicles, rather than as a universal replacement for all OBD-II-based solutions. Its main advantage lies in enabling preventive-maintenance digitization when independence from the ECU, the diagnostic port, and smartphone pairing is operationally desirable. Validation of SMS messaging as the exclusive alert channel confirmed its economic sustainability. With reduced operating costs (75–85% savings), the system is accessible to the average user and small transportation fleets, aligning with the need to reduce the high costs associated with unplanned corrective maintenance.

For vehicles with reliable diagnostic-port access, future work will evaluate hybrid configurations that combine OBD-II data acquisition and Bluetooth/app-based visualization with the standalone preventive-maintenance logic developed in this study. In parallel, the development of a complementary mobile application capable of accessing the maintenance history stored in the system and presenting it through a graphical interface will also be

explored. A further line of work will consist of logging the mileage driven between the first warning and the subsequent maintenance reset, so that the system can estimate the user's typical response lag and dynamically adjust the initial alert threshold in a more personalized and adaptive manner. Future work will also include validation on a broader range of vehicle makers, ages, and electrical architectures in order to assess how robustly the proposed system can be generalized beyond the representative vehicle used in the present study.

Author Contributions: Writing—review and editing, J.B.-Z.; Investigation, J.M.-P.; Methodology, R.L.-C. All authors have read and agreed to the published version of the manuscript.

Funding: This research received no external funding and the APC was funded by Politecnica Salesiana university.

Data Availability Statement: The original contributions presented in this study are included in the article. Further inquiries can be directed to the corresponding author.

Conflicts of Interest: The authors declare no conflicts of interest.

Appendix A. Complete Circuit Diagram

The circuit design was performed using Fritzing software, enabling pre-simulation of the system before physical implementation. Figure A1 presents the complete system schematic, showing connections between the Arduino Mega 2560 microcontroller and peripheral modules (GPS, GSM, MicroSD, and voltage sensor).

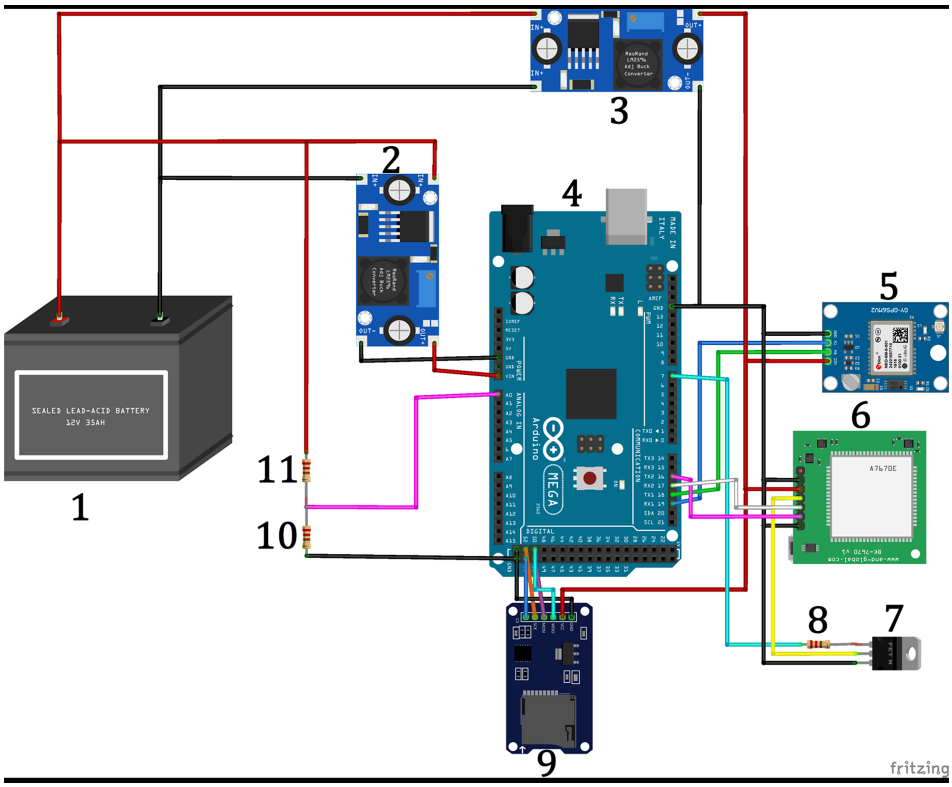

Figure A1. Complete schematic diagram of the preventive maintenance management system simulated in Fritzing. Parts: 1 (12V vehicle battery), 2 and 3 (voltage converter), 4 (Arduino Mega), 5 (GPS module), 6 (GSM module), 7 (MOSFET), 8 (resistor), 9 (MicroSD module), 10 and 11 (resistors).

Table A1. System connections.

Component	Component Pin	Destination Device	Destination Pin
GPS Module	GND	Arduino Mega	GND
GPS Module	VCC	Voltage conv. #3	OUT+
GPS Module	TX	Arduino Mega	RX(19)
GPS Module	RX	Arduino Mega	TX(18)
GSM Module	GND	Arduino Mega	GND
GSM Module	VCC	Voltage conv. #3	OUT+
GSM Module	RX	Arduino Mega	TX2(16)
GSM Module	TX	Arduino Mega	RX2(17)
GSM Module	PWRKEY	MOSFET	Drain
MicroSD Module	CS	Arduino Mega	53
MicroSD Module	MOSI	Arduino Mega	51
MicroSD Module	MISO	Arduino Mega	50
MicroSD Module	SCK	Arduino Mega	52
MicroSD Module	VCC	Voltage conv.	OUT+
MicroSD Module	GND	Arduino Mega	GND
MOSFET	Gate	Arduino Mega	7
MOSFET	Source	Arduino Mega	GND

Appendix B. Component List and Technical Specifications

Component selection was made considering the criteria of commercial availability, voltage compatibility, energy consumption, and operational reliability. Table A2 details all electronic components used in the prototype, including the model, relevant technical specifications, and quantity used.

Table A2. Electronic components of the system.

N°	Component	Qty.	Unit Cost (USD)	Subtotal (USD)
1	Arduino Mega 2560	1	$25.00	$25.00
2	Jumper cables	40	$0.05	$2.00
3	GPS antenna	1	$10.25	$10.25
4	Protoboard	1	$1.91	$1.91
5	Ring terminals	2	$0.15	$0.30
6	DC connectors	2	$0.45	$0.90
7	AWG cable	1	$4.00	$4.00
8	Resistors	3	$0.05	$0.15
9	LM2596S voltage converter module	2	$2.50	$5.00
10	GSM Module A7670SA	1	$10.17	$10.17
11	GPS Module Ublox Neo 6M	1	$5.95	$5.95
12	MicroSD module	1	$1.81	$1.81
13	MicroSD 64 GB	1	$6.90	$6.90
14	Enclosure	1	$3.00	$3.00
15	MOSFET irf540N	1	$1.50	$1.50
			TOTAL	$78.84

Appendix C. Physical Prototype Assembly

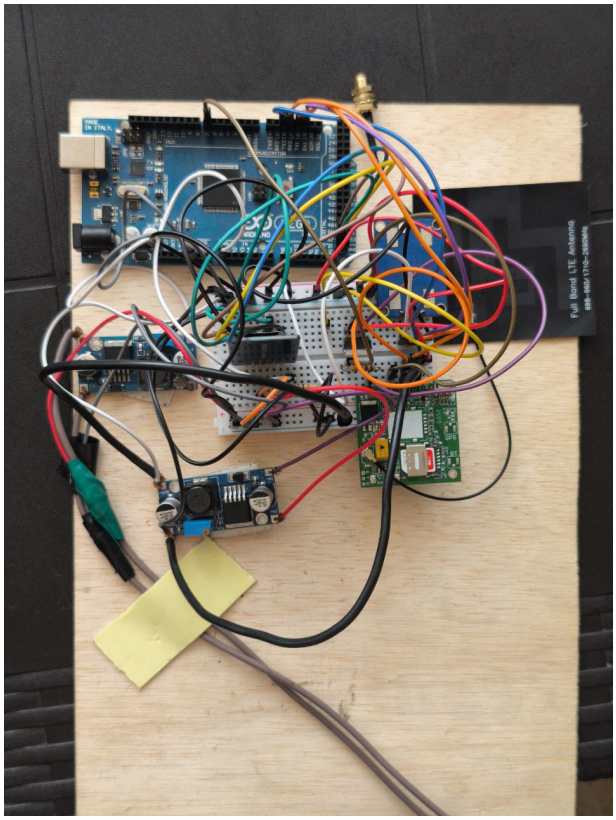

Figure A2. Physical assembly of the implemented prototype.



Figure A3. Field route test of the prototype.



Figure A4. Battery connection.



Figure A5. Connector output to the vehicle cabin.

Appendix D. General Code Structure

This appendix presents the complete and final source code of the firmware implemented in the Arduino Mega 2560 microcontroller. The system has been programmed with a dynamic architecture that includes a state machine for interactive configuration via SMS messages. This allows the user to select their vehicle from a pre-loaded database (`DATA.CSV`) and automatically manage multiple maintenance intervals without requiring physical hardware reprogramming.

Listing A1. General firmware architecture implemented in the Arduino Mega 2560 microcontroller.

```
// 1. GLOBAL VARIABLES AND DYNAMIC STRUCTURES
float batteryVoltage = 0.0;
bool engineOn = false, isConfigured = false;
unsigned long totalOdometer = 0;
const int NUM_MAINT = 6;
String maintNames[NUM_MAINT];
unsigned long maintIntervals[NUM_MAINT], maintCounters[NUM_MAINT];
```

Listing A1. *Cont.*

```
// State machine for interactive configuration
enum SetupState {
  ST_IDLE, ST_WAIT_MODEL_INDEX, ST_WAIT_ODO, ST_WAIT_HISTORY
};
SetupState setupState = ST_IDLE;

// 2. VIRTUAL IGNITION AND SATELLITE ODOMETRY
void readVoltage() {
  batteryVoltage = (analogRead(PIN_VOLT) * 5.0 / 1023.0) * 5.7;
  engineOn = (batteryVoltage > 13.8);
}
/* Main loop: urban noise filter and accumulation
if (gps.speed.kmph() > 3.0 && distMeters > 5.0) {
  totalOdometer += distMeters;
  for (int i = 0; i < NUM_MAINT; i++)
    maintCounters[i] += distMeters;
} */

// 3. STATE MACHINE FOR SMS CONFIGURATION
void processIncomingSMS(String sender, String text) {
  if (!isConfigured) {
    switch(setupState) {
      case ST_IDLE:
        sendModelListSMS();
        setupState = ST_WAIT_MODEL_INDEX; break;
      case ST_WAIT_MODEL_INDEX:
        /* Extracted model selection logic... */
        setupState = ST_WAIT_ODO; break;
      case ST_WAIT_ODO:
        totalOdometer = text.toInt() * 1000UL;
        setupState = ST_WAIT_HISTORY; break;
      case ST_WAIT_HISTORY:
        maintCounters[setupMaintIndex++] = text.toInt() * 1000UL;
        if (setupMaintIndex >= NUM_MAINT) {
          isConfigured = true;
          saveConfig();
        }
        break;
    }
  }
}

// 4. ALERT ENGINE AND PERSISTENCE (MicroSD)
/* Periodic check routine (executed in loop)
for (int i = 0; i < NUM_MAINT; i++) {
  long remKm = (maintIntervals[i]-maintCounters[i])/1000;
  if (remKm<=50 && remKm>10)
    sendSMS("ALERT: "+maintNames[i]+" in 50 km.");
  else if (remKm<=10 && remKm>0)
    sendSMS("URGENT: "+maintNames[i]+" in 10 km.");
  else if (remKm<=0)
    sendSMS("OVERDUE: "+maintNames[i]+".");
} */
void saveConfig() {
  File file = SD.open("CONFIG.TXT", FILE_WRITE);
  // Persists: phone, vehicle, odometer, maintenance counters
  file.close();
}
```

* Adapted excerpt from the complete source code.

Appendix E. Experimental Data Obtained

Table A3. Summary of statistical performance indicators and error by test scenario.

Test Scenario	N	Mean Error (Bias) [km]	Std. Dev. (*S*) [km]	RMSE [km]	MAPE [%]
Route A (Urban)	5	+0.710	0.035	0.711	6.45%
Route B (Peripheral)	5	+0.854	0.024	0.854	2.08%
Route C (Interurban)	11	+1.088	0.016	1.088	3.40%
Global Average	21	+0.942	0.166	0.956	3.98%

Agreement between the prototype and the vehicle odometer was additionally evaluated using a route-specific Bland–Altman analysis, since this approach is more informative for method-agreement assessment than hypothesis testing alone. Because each scenario involved a fixed route length, the analysis was performed separately for the urban, peripheral, and interurban routes [33].

Table A4. Detailed log of alert transmission latency times ($N = 20$).

Test No.	Latency (s)	Test No.	Latency (s)
1	4.67	11	3.94
2	4.19	12	3.94
3	4.78	13	4.47
4	5.00	14	3.00
5	4.12	15	3.00
6	4.12	16	3.87
7	5.00	17	3.53
8	4.87	18	4.53
9	3.94	19	3.61
10	4.70	20	3.23

Mean = 4.13 s; Std. Dev. = 0.63 s; Max = 5.00 s.

Table A5. Bland–Altman agreement statistics between the prototype and the vehicle odometer by route type. Bias is defined as Prototype minus Odometer.

Scenario	N	Mean Bias (km)	SD (km)	Lower LoA (km)	Upper LoA (km)
Route A (Urban)	5	+0.710	0.035	+0.641	+0.779
Route B (Peripheral)	5	+0.854	0.024	+0.807	+0.901
Route C (Interurban)	11	+1.088	0.016	+1.057	+1.120

Shapiro–Wilk Normality Tests and Bland–Altman Plots:

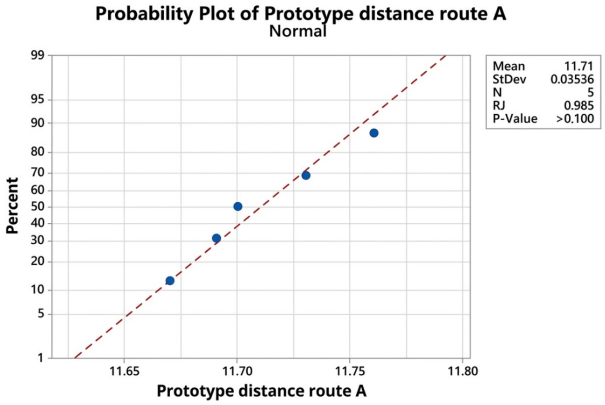

Figure A6. Shapiro–Wilk normality test—Route A ($p > 0.100$).

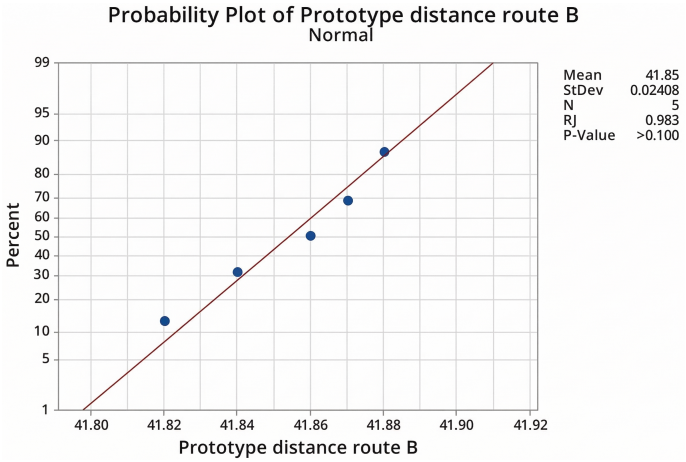

Figure A7. Shapiro–Wilk normality test—Route B ($p > 0.100$).

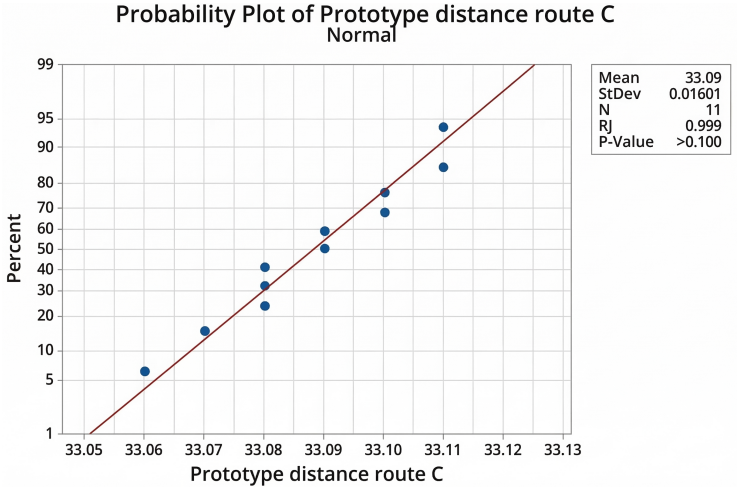

Figure A8. Shapiro–Wilk normality test—Route C ($p > 0.100$).

Bland–Altman Method-Agreement Plots

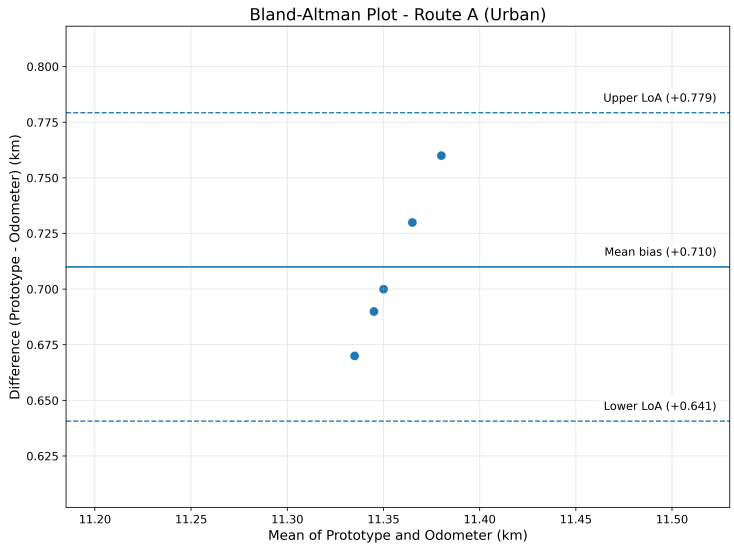

Figure A9. Bland–Altman plot—Route A (Urban). Mean bias = +0.710 km; 95% limits of agreement: +0.641 to +0.779 km.

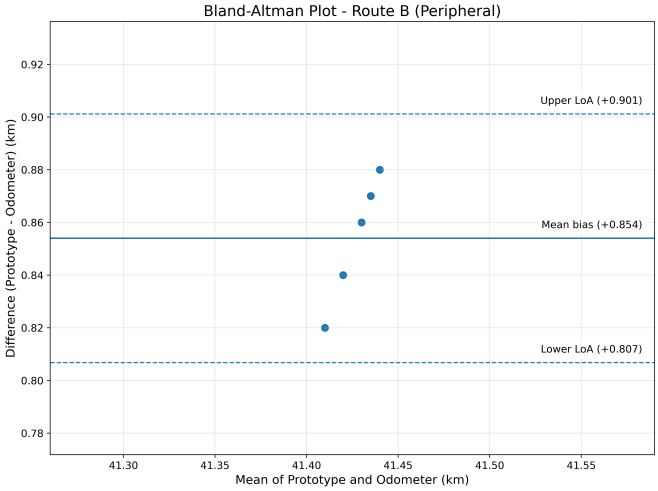

Figure A10. Bland–Altman plot—Route B (Peripheral). Mean bias = +0.854 km; 95% limits of agreement: +0.807 to +0.901 km.

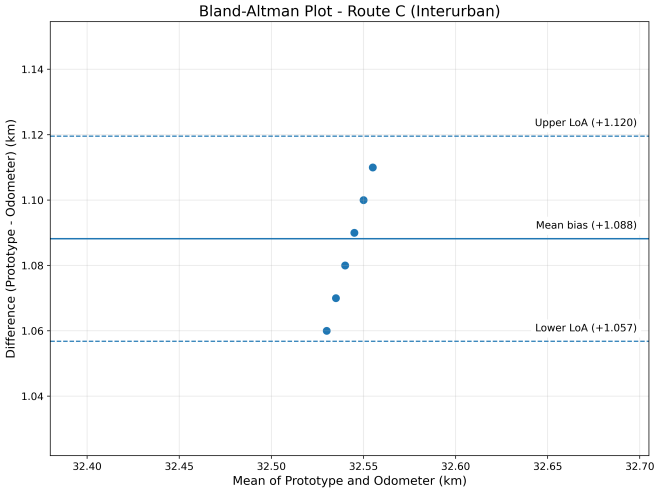

Figure A11. Bland–Altman plot—Route C (Interurban). Mean bias = +1.088 km; 95% limits of agreement: +1.057 to +1.120 km.

References

1. World Health Organization. *Global Status Report on Road Safety 2023*; WHO: Geneva, Switzerland, 2023. Available online: https://iris.who.int/handle/10665/375016 (accessed on 5 December 2025).
2. Asociación de Empresas Automotrices del Ecuador (AEADE). *Anuario del Sector Automotriz 2023*; AEADE: Quito, Ecuador, 2023. Available online: https://www.aeade.net/ (accessed on 5 December 2025).
3. Soon, T.W.; Osman, Z.; Nafis, M. Investigation of accuracy and response time in GPS-based car mileage monitoring device. *Mekatronika* **2022**, *4*, 1–7. [CrossRef]
4. Lino, G.V.; Arriaga, J. Análisis de Eficacia de un Modelo de Gestión para Mantenimiento Preventivo de Vehículos en la Policía de Santa Elena. Polo del Conocimiento. 2025. Available online: https://polodelconocimiento.com/ojs/index.php/es/article/view/8671 (accessed on 16 December 2025).
5. Instituto Ecuatoriano de Normalización (INEN). *RTE-002: Reglamento Técnico Ecuatoriano de Emisiones de Vehículos Automotores*; INEN: Quito, Ecuador, 1996. Available online: https://www.normalizacion.gob.ec/buzon/reglamentos/RTE-002.pdf (accessed on 16 December 2025).
6. López-Chila, R.; Abad-Reyna, H.; Morocho-Cajas, J.; Fierro-Jiménez, P. Development of representative urban driving cycles for congested traffic conditions in Guayaquil using real-time OBD-II data and weighted statistical methods. *Vehicles* **2025**, *7*, 95. [CrossRef]
7. Hussain, S.M.; Yang, U.; Shunkun. Car e-Talk: An IoT-enabled cloud-assisted smart fleet maintenance system. *IEEE Internet Things J.* **2021**, *8*, 1234–1245. [CrossRef]
8. Giraldo, M.; Huertas, J.I. Real emissions, driving patterns and fuel consumption of in-use diesel buses operating at high altitude. *Transp. Res. Part D* **2019**, *77*, 21–36. [CrossRef]

9. Sanasie, G.; Radzak, Z.I.A.; Zakaria, M.A. Preventive maintenance data logger monitoring system. *Mekatronika* **2021**, *3*, 1–6. [CrossRef]
10. Myszkowski, S.; Burnos, A.; Gnap, J.; Poliak, M. Modeling Vehicle Fuel Consumption Using a Low-Cost OBD-II Interface. *Energies* **2023**, *16*, 7266. [CrossRef]
11. Soy, H. Coverage Analysis of LoRa and NB-IoT Technologies on LPWAN-Based Agricultural Vehicle Tracking Application. *Sensors* **2023**, *23*, 8859. [CrossRef]
12. Farré, V.; Vega-Sánchez, J.; Garzón, V.; Garzón, N.O.; Mora, H.C.; Benitez-Olivo, E.E. Design and performance analysis of sub-THz/THz mini-cluster architectures for dense urban 5G/6G networks. *Sensors* **2025**, *25*, 6717. [CrossRef] [PubMed]
13. Addo, P.A.; Dwomoh, L.; Ofori, C. Automatic maintenance alert system for heavy duty haulage machines. *J. Nas. Tek. Elektro* **2022**, *11*, 1–8. [CrossRef]
14. Hernández-Sampieri, R.; Mendoza, C. *Metodología de la Investigación: Las Rutas Cuantitativa, Cualitativa y Mixta*; McGraw-Hill: Mexico City, Mexico, 2018.
15. Nguyen, K.T.P.; Medjaher, K. A new dynamic predictive maintenance framework using deep learning for failure prognostics. *Reliab. Eng. Syst. Saf.* **2019**, *188*, 251–262. [CrossRef]
16. Zhang, P.; Gao, Z.; Cao, L.; Dong, F.; Zou, Y.; Wang, K.; Zhang, Y.; Sun, P. Marine systems and equipment prognostics and health management: A systematic review. *Machines* **2022**, *10*, 72. [CrossRef]
17. Einabadi, B.; Mahmoodjanloo, M.; Baboli, A.; Rother, E. Dynamic predictive and preventive maintenance planning in the automotive industry. *J. Manuf. Syst.* **2023**, *69*, 292–310. [CrossRef]
18. National Institute of Standards and Technology (NIST). *Handbook 44: Specifications, Tolerances, and Other Technical Requirements for Weighing and Measuring Devices*; NIST: Washington, DC, USA, 2023. [CrossRef]
19. Alomari, A.H.; Khedaywi, T.S.; Marian, A.R.O.; Jadah, A.A. Traffic Speed Prediction Techniques in Urban Environments. *Heliyon* **2022**, *8*, e11847. [CrossRef]
20. Kondaveeti, H.K.; Kumaravelu, N.K.; Vanambathina, S.D.; Mathe, S.E.; Vappangi, S. A systematic literature review on prototyping with Arduino. *Comput. Sci. Rev.* **2021**, *40*, 100364. [CrossRef]
21. Hernández-Rodríguez, E.; González-Rivero, R.A.; Schalm, O.; Martínez, A.; Hernández, L.; Alejo-Sánchez, D.; Janssens, T.; Jacobs, W. Reliability testing of a low-cost multi-purpose Arduino-based data logger. *Sensors* **2023**, *23*, 7412. [CrossRef] [PubMed]
22. U-blox AG. *NEO-M8 Series GNSS Modules Data Sheet*; U-blox: Thalwil, Switzerland, 2021. Available online: https://www.u-blox.com/en/product/neo-m8-series (accessed on 16 December 2025).
23. Menaka, M.; Tharani, R.; Pemila, M.; Bhavana, H. GSM-based vehicle anti-theft and maintenance alert device using vibration sensor and Arduino. In Proceedings of the International Conference on Data Science and Business Systems (ICDSBS), Chennai, India, 17 April 2025. [CrossRef]
24. Navixy. SMS in GPS Tracking and Transport Telematics as Vital as GPRS. 2020. Available online: https://www.navixy.com (accessed on 16 December 2025).
25. Hyundai. Hyundai Accent 2012 Owner's Manual. Scheduled Maintenance Service Section, Normal Maintenance Schedule. 2012. Available online: https://www.manual.ec/hyundai/accent-2012/manual (accessed on 20 December 2025).
26. Fawcett, T. An introduction to ROC analysis. *Pattern Recognit. Lett.* **2006**, *27*, 861–874. [CrossRef]
27. Zhang, H.; Zhang, R.; Sun, J. Developing real-time IoT-based public safety alert and emergency response systems. *Sci. Rep.* **2025**, *15*, 13465. [CrossRef]
28. Althoubi, A.; Alshahrani, R.; Peyravi, H. Delay analysis in IoT sensor networks. *Sensors* **2021**, *21*, 3876. [CrossRef]
29. Ranacher, P.; Brunauer, R.; Mackaness, W.A.; Van der Spek, S. Why GPS makes distances bigger than they are. *Int. J. Geogr. Inf. Sci.* **2016**, *30*, 316–333. [CrossRef]
30. Lopez-Chila, R.; Abad-Correa, A.; Cruz-Zavala, H. Analysis of the influence of driving modes in a hybrid vehicle on fuel consumption optimization. *Int. J. Innov. Res. Soc. Sci.* **2025**, *8*, 6017. [CrossRef]
31. Agencia Nacional de Tránsito (ANT). *Estadísticas de Siniestralidad de Tránsito: Anuario 2024*; ANT: Quito, Ecuador, 2024. Available online: https://www.ant.gob.ec (accessed on 16 December 2025).
32. Ashik, F.R.; Rahman, M.H.; Zafri, N.M.; Antipova, A.; Labib, S.M. Car Ownership, Commute Distance, and Commute Mode Choice in the Dense Megacity of a Developing Country: The Direct and Indirect Role of the Built Environment. *Transp. Res. Rec. J. Transp. Res. Board* **2024**, *2678*, 1923–1938. [CrossRef]
33. Bland, J.M.; Altman, D.G. Statistical methods for assessing agreement between two methods of clinical measurement. *Lancet* **1986**, *327*, 307–310. [CrossRef]

Disclaimer/Publisher's Note: The statements, opinions and data contained in all publications are solely those of the individual author(s) and contributor(s) and not of MDPI and/or the editor(s). MDPI and/or the editor(s) disclaim responsibility for any injury to people or property resulting from any ideas, methods, instructions or products referred to in the content.